Weierstraß–Institut
für Angewandte Analysis und Stochastik

im Forschungsverbund Berlin e.V.

Preprint ISSN 0946 – 8633

On the Dynamics of Single Mode Lasers with Passive Dispersive Reflector

Vasile Tronciu[1 2], Hans-Jürgen Wünsche[1], Jan Sieber [3],

Klaus Schneider[3], Fritz Henneberger[1]

submitted: 15th December 1999

[1] Institut für Physik
der Humboldt-Universität zu Berlin,
Invalidenstr. 110, 10115 Berlin, Germany
E-Mail: tronciu@physik.hu-berlin.de
E-mail: wuensche@physik.hu-berlin.de
E-mail: henneberger@physik.hu-berlin.de

[2] Technical University of Moldova
Department of Physics
Stefan cel Mare av. 168,
Chisinau MD-2004, Moldova
E-mail tronciu@mail.utm.md

[3] Weierstraß-Insitut für Angewandte
Analysis und Stochastik,
Mohrenstraße 39, 10117 Berlin, Germany
E-Mail: sieber@wias-berlin.de
E-Mail: schneider@wias-berlin.de

Preprint No. 541
Berlin 1999

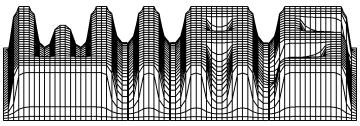

1991 Mathematics Subject Classification. 78A60, 78-05, 78A55.

Key words and phrases. Semiconductor laser, DFB lasers, Self-Pulsations.

Edited by
Weierstraß–Institut für Angewandte Analysis und Stochastik (WIAS)
Mohrenstraße 39
D — 10117 Berlin
Germany

Fax: + 49 30 2044975
E-Mail (X.400): c=de;a=d400-gw;p=WIAS-BERLIN;s=preprint
E-Mail (Internet): preprint@wias-berlin.de
World Wide Web: http://www.wias-berlin.de/

Abstract

For passive dispersive reflector (PDR) lasers we investigate a single mode model containing two functions characterizing the influence of the PDR. We study numerically the effect of the shape of these functions on the existence and robustness of self-pulsations. The possibility of tuning the frequency and modulation depth of the self-pulsations has been demonstrated.

1 Introduction

Multi-section DFB-lasers can exhibit self-pulsations (SP) [1]-[12]. SP of dispersive self Q-switching (DQS) type have been studied both experimentally [2] -[6], [11],[12] and theoretically [7] -[10], [12] for lasers containing two active DFB-sections.
Although the basic mechanisms for the generation of these SP are well understood, it is still a challenge to find design rules for tailoring the parameters of the SP such as the repetition frequency and the pulse shape. Especially, the question in which range the SP parameters can be varied by changing the device parameters (section lengths, grating period) is crucial for applications.
Since the calculations of the transient behaviour of a multi-section DFB-lasers by means of the TDE model [17] is rather time consuming and since the number of device parameter to be taken into account is high, in the following we introduce a single mode model containing only a few parameters. The derivation of this model is based on two important simplifications.
First, we profit from the fact that the DFB-section serving as dispersive reflector is usually kept close to the gain transparency. Therefore, the carriers of this section couple only weakly to the photons. Taking into account this effect we completely replace the reflector by a passive section, as sketched in Figure 1.

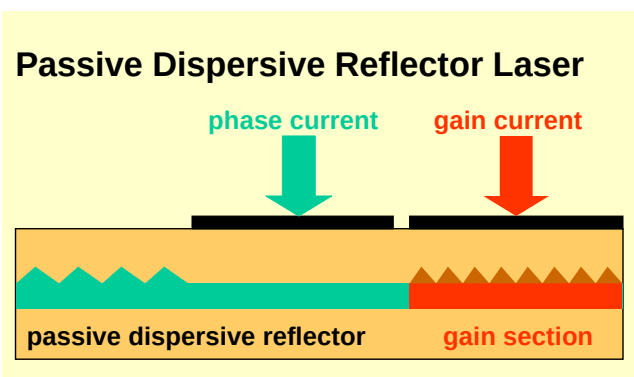

Fig. 1: Scheme of a passive dispersive reflector (PDR) laser. Only the carriers in the gain section couple to the optical field. The waveguide in the PDR sections is passive. The example sketched here consists of a phase tuning section and a DFB-section.

In this modelling a PDR-laser has only one active DFB-section. The passive part of the device may consist of different phase and reflector sections. Furthermore, chirped gratings allow a nearly arbitrary tuning of the reflector properties.
Our *second simplification* is based on the observation that in the frame of the single mode model all the many device parameters enter only few functions of the carrier density (gain, losses, fill & Petermann factors). We call these functions rate equation (RE) functions. It seems natural to consider the RE-functions as the basic characteristics determining the nature of the SP. This allows us to split the tailoring procedure into two almost independent steps. In a first step, we have to find such RE-functions providing the desired properties of the SP of a PDR-laser. In the next step the properties of the PDR must be tailored for obtaining the appropriate RE-functions.
The goal of our study is to demonstrate that the SP frequency of a PDR-laser depends strongly on the parameters of the passive dispersive reflector. The paper is organised as follows. In Section 2 we derive some normal form for a system of two rate equations containing only two RE-functions. Furthermore, we present a typical pair of RE-functions. Section 3 contains a stability analysis of the stationary states in dependence on the PDR parameters. In Section 4 we study the generation of SP via Hopf bifurcation and we apply a continuation method to compute the periodic solutions. The influence of the PDR parameters on the self-pulsation frequency and on the modulation depth is discussed in Section 5. A summary and conclusions are given in Section 6.

2 Mode Equations

2.1 The single mode rate equations

We start from the rate equations presented in [12]. In our case of a PDR -laser, only one DFB-section is active. Therefore, the carrier number N in this section and the photon number S are the dynamic variables, and the equations read

$$\frac{dN}{dt} = \frac{I}{e} - \frac{N}{\tau_e} - v_g \Gamma g S, \tag{1}$$

$$\frac{d}{dt}\left(\frac{S}{\sqrt{K_z}}\right) = \left(v_g \Gamma g - \gamma_p\right)\left(\frac{S}{\sqrt{K_z}}\right), \tag{2}$$

where e is the elementary charge, v_g the group velocity, I the injection current into the gain section and τ_e the spontaneous life-time of carriers.
For the modal gain g we use the simple linear approximation

$$g(N) = g'\left(N - N_{tr}\right), \tag{3}$$

where g' is the differential gain and N_{tr} is the transparency concentration. Furthermore, $\Gamma(N)$ is a *longitudinal* fill factor, i.e., the relative part of power contained in the gain section[1], $\gamma_p(N)$ is the optical loss rate due to the radiation emitted at the facets and due to the internal losses, and $K_z(N)$ is the longitudinal analogy to Petermann's K-factor of the excess spontaneous emission [14].
Under our assumption that the carrier numbers change only in one part of the device, the functions $\Gamma(N), \gamma_p(N)$ and $K_z(N)$ may exhibit considerable variations with changing carrier number N. A detailed description of the calculation of these functions by means of the coupled mode equations has been given in previous papers [7, 12, 15].

2.2 Transformation to normal form

As mentioned in the introduction, many parameters enter the rate equations in the single mode model. In this section we transform the rate equations (1)-(2) to some normal form.
Let N_{th} be the smallest zero of the function $v_g\Gamma(N)g(N) - \gamma_p(N)$. N_{th} is called the threshold carrier number. By means of the nonlinear coordinate transformation

$$n = \frac{N - N_{th}}{N_{th} - N_{tr}}, \qquad p = v_g g' \tau_e \Gamma(N_{th}) \frac{\sqrt{K_z(N_{th})}}{\sqrt{K_z(N)}} \frac{S}{N_{th} - N_{tr}}$$

we introduce the quasi-carrier number n and the quasi-photon number p as new variables. In these variables the rate equations (1)-(2) read as follows

$$\frac{dn}{d\tau} = \mathcal{J} - n - (1+n)K(n)p, \tag{4}$$

$$\frac{dp}{d\tau} = G(n)p \tag{5}$$

with

$$G(n) = T\left[\frac{\Gamma(n)}{\Gamma(N_{th})}(1+n) - \frac{\gamma_p(n)}{\gamma_p(N_{th})}\right], \tag{6}$$

$$K(n) = \frac{\Gamma(n)}{\Gamma(N_{th})}\sqrt{\frac{K_z(N)}{K_z(N_{th})}}, \tag{7}$$

where $\mathcal{J} = (I - I_{th})/(I_{th} - I_{tr})$ is the relative excess injection rate, $\tau = t/\tau_e$ is the dimensionless time and $T = \gamma_p^{th}\tau_e$ is the dimensionless photon loss rate. Here $I_{tr} = eN_{tr}/\tau_e$ and $I_{th} = eN_{th}/\tau_e$ are the transparency and threshold currents, respectively.

[1] This differs from the common notation where Γ is used for the *transverse* confinement factor, which we assume to be included in g, for brevity.

The equations (4)-(7) describe the single mode dynamics of a laser consisting of one active section and an arbitrary passive reflector.
Typically we have $\gamma_p^{th} = 5 \cdot 10^{11}\mathrm{s}^{-1}$, thus we find the following orders of magnitude

$$T \sim 500, \quad 0 < \mathcal{J} < 10, \qquad |n| \ll 1.$$

The most simple case is that without reflector, i.e., a solitary active DFB-section. In this situation, Γ, K_z and γ_p are independent of the carrier number such that we have

$$\Gamma(n) \equiv K(n) \equiv 1, \qquad G(n) \equiv Tn. \tag{8}$$

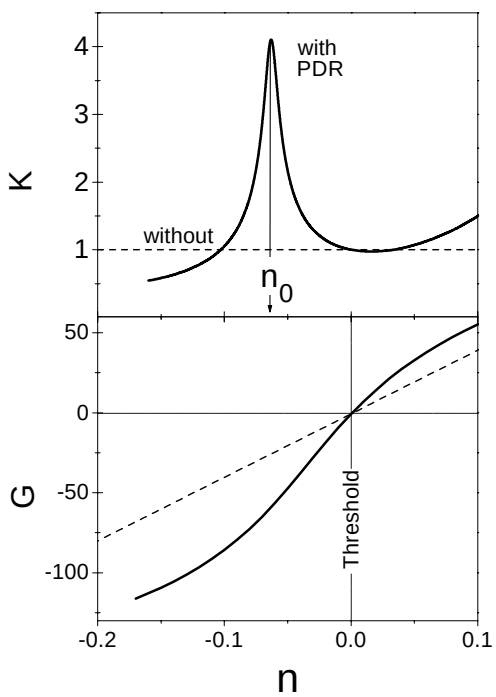

Fig. 2: Typical profile of the RE functions $K(n)$ and $G(n)$ for a solitary gain section (dashed lines) and for PDRL (solid lines).

The plots of these functions are shown in Figure 2 (dashed lines). Thus, any single section DFB-laser can be described by the reduced rate equations with only two parameters, the excess injection $\mathcal{J}$ and T.

A dispersive reflector influences the dynamics via the shape of the two functions $K(n), G(n)$, which are the RE-functions discussed in the introduction. In case of a single section reflector with a uniform index coupled grating, examples for the carrier density dependence on the quantities composing the RE functions (Γ, γ_p, K_z) can be found in [7, 10]. The most prominent feature is a narrow resonance-like enhancement of K_z which implies a corresponding resonance of $K(n)$. This resonance is closely related to the appearence of a mode degeneracy at the point where K_z diverges [10]. We believe that such a resonance of K_z due to a mode degeneracy is a rather general consequence of dispersive reflectors. This phenomenon has also been obtained in [12] for more complicated reflectors composed of a DFB-section accomplished by a phase tuning section.

Using the formula and parameter values for a conventional DFB-laser described in [12], [15], [17] we have calculated the RE functions for devices with similar reflector structures. A typical example of a function representing the resonance structure of $K(n)$ is drawn in Figure 2 (solid line). The position of the resonance, its width and height vary in dependence on the parameters of the reflector. To study the consequences of these different configurations on the dynamics, we shall use the following

simple Lorentzian model for the resonance

$$K(n) = K_0 + \frac{AW^2}{4(n-n_0)^2 + W^2} \tag{9}$$

where n_0 (detuning) determines the position of the resonance, A is its amplitude and W its width. In the sequel we set K_0 such that $K(0) = 1$ which is consistent with (7).
The influence of different reflectors on the RE-function $G(n)$ is mainly an enhancement of its slope within a finite interval. For the following investigations, this feature will be modeled by the simple function

$$G(n) = T\left(n + \alpha \cdot \Delta \cdot \tanh\left(\frac{n}{\Delta}\right)\right). \tag{10}$$

The parameters Δ and α characterize the width of the slope enhancement region and the magnitude of the relative slope enhancement, respectively.

3 Stability of the equilibria

System (4)-(5) has two stationary solutions,

$$(n_1, p_1) = \left(0, \frac{\mathcal{J}}{K(0)}\right) \quad \text{[laser "on"]}, \tag{11}$$

$$(n_2, p_2) = (\mathcal{J}, 0) \quad \text{[laser "off"]}. \tag{12}$$

To determine the stability of these solutions we compute the eigenvalues of the Jacobian of the right-hand side of (4)-(5) at these points.
The eigenvalues at the off-state are

$$\lambda_1^{\text{off}} = -1 - K(\mathcal{J}), \quad \lambda_2^{\text{off}} = G(\mathcal{J}).$$

Since $G(\mathcal{J}) > 0$ for $\mathcal{J} > 0$ the off-state is unstable above threshold.
In what follows we focus on the on-state which has a physical sense only for $\mathcal{J}/K(0) > 0$. Its stability is governed by the pair of complex eigenvalues

$$\lambda_{\pm}^{\text{on}} = -\gamma \pm i\sqrt{\omega^2 - \gamma^2}$$

where γ expresses the damping γ and ω the frequency

$$\gamma = \frac{1}{2}\left[1 + \left(1 + \frac{K'(0)}{K(0)}\right)\mathcal{J}\right], \quad \omega^2 = G'(0)\mathcal{J}. \tag{13}$$

In case of a solitary gain section described by (8) the on-state (n_1, p_1) is a stable focus with damping $\gamma = (1+\mathcal{J})/2$ and frequency $\omega = \sqrt{T\mathcal{J}}$ provided $\omega^2 > \gamma^2$.

The expressions in (13) describe the influence of the values $K'(0)/K(0)$ and $G'(0)$ on the damping γ and the frequency ω.
Now we study how the stability of the on-state depends on the parameters A and n_0 for fixed W. A simple analysis shows that the damping γ as a function of n_0 has at most two roots for any A and W. If A is sufficiently large, the function $\gamma(n_0)$ has two simple zeroes, its graph is shown in Figure 3 (solid line). This curve visualizes that the resonance of $K(n)$ affects the stability of the on-state only if its position is within an interval near threshold. In this region the damping is strongly enhanced for $n_0 > 0$. For large A and decreasing n_0 the stability of the on-state changes rapidly near $n_0 = 0$ from a strongly damped focus to a strongly unstable focus. For $|n_0| \gg W$ the resonance of $K(n)$ does not influence the damping of the on-state. It is as small as without PDR (dashed line in Figure 3). We conclude that the introduction of a PDR changes essentially the behaviour of damping.

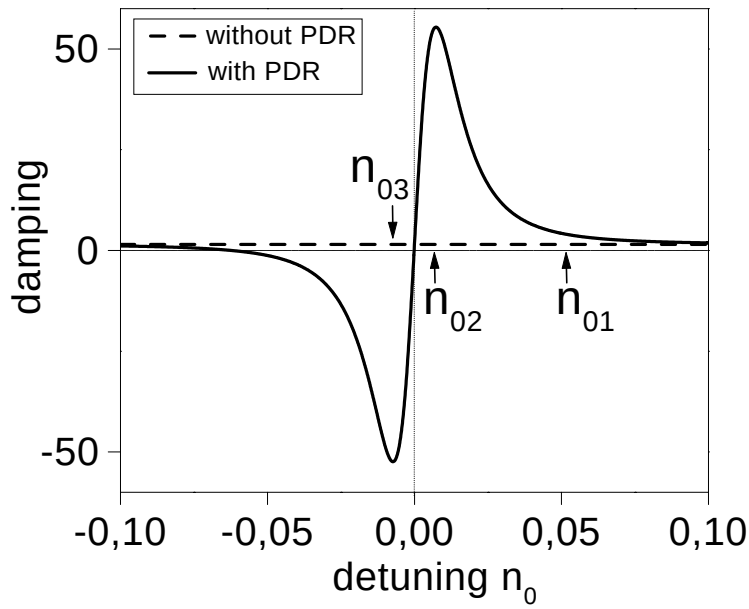

Fig. 3: Dependence of γ on the detuning n_0 for a solitary gain section (dashed line) and for a gain section with a passive dispersive reflector (solid line) ($W = 0.02, A = 1, \mathcal{J} = 2$).

One of the basic functions of optical devices is the optical switching between stable steady states. Now we demonstrate how the region of enhanced positive damping can be used to design an optical switching device. To this purpose we apply an external injected current of step type

$$\mathcal{J} = \begin{cases} 1 & : \quad 0 \leq \tau \leq 0.5 \\ 2 & : \quad 0.5 < \tau < 1 \end{cases}$$

and solve the initial value problem (4)-(5) with (9), (10) starting from the on-state for different detuning $n_0 = n_{01} = 0.05$ and $n_0 = n_{02} = 0.005$.

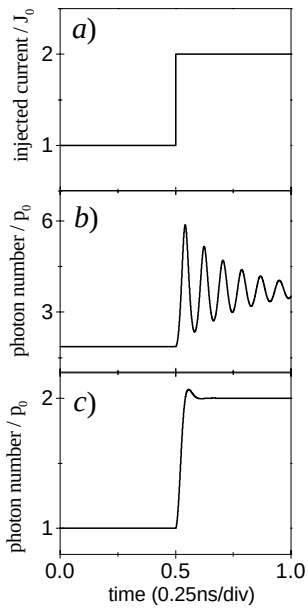

Fig. 4: Time behaviour of the injected current a). Dynamic response of PDRL for different detuning values b) $n_{01} = 0.05$ (damping of the solitary gain section), c) $n_{02} = 0.005$ (enhanced damping); where $W = 0.02, A = 1$, $\alpha = 5, \Delta = 0.1$. $\mathcal{J}_0 = e(N_{th} - N_{tr})/\tau_e$.

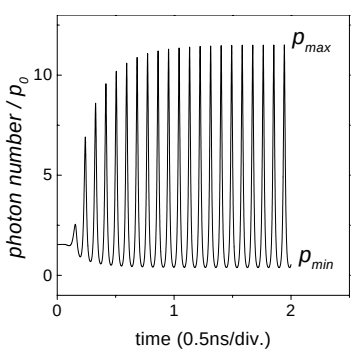

Fig. 5: Time evolution of photon number/p_0 for negative damping and detuning value $n_{03} = -0.005$ (region of SP), where $\mathcal{J} = 2$, $W = 0.02, A = 1$, $\alpha = 5, \Delta = 0.1$.

Figures $4^{b,c}$ show the time behaviour of p/p_0 ($p_0 = (N_{th} - N_{tr})/(v_g g' \tau_e)$) for two different values of detuning: n_{01} corresponds to the damping of the solitary gain section and n_{02} to enhanced damping (Fig. 3). Figure 4^b shows the temporal evolution of photon number/p_0 calculated numerically for $n_0 = n_{01}$. The most important feature of this transient response is that the switching is accompanied by weakly damped oscillations. These oscillations are referred to as relaxation oscillations.

Figure 4^c represents the influence of enhanced damping on the switching properties. In case $n_0 = n_{02}$ and when the injected current changes from $\mathcal{J} = 1$ to $\mathcal{J} = 2$ the transient response practically reflects the form of the injected current such that the switching time is shorter by 2 orders of magnitude compared with the previous case.

From the Figures $4^{b,c}$ it is evident that the passive dispersive reflector leads to the increase of the damping and strongly reduces the switching time between stationary states. For negative detuning $n_0 = n_{03}$ (see Fig. 3) the stationary state corresponding to $\mathcal{J}$=2 is unstable and we observe self-pulsations (Fig. 5). The nature of these self-pulsations is discussed in the following section.

We would like to emphasize that for a detuning n_0 near the threshold a PDRL shows two different kinds of dynamic behaviour: fast response without relaxation oscillations (fast switching) for small positive n_0 and self-pulsations for negative detuning.

4 Bifurcation Analysis

In the previous section we have shown that the on-state is unstable for sufficiently large amplitude A if the detuning n_0 belongs to some interval $B_2 < n_0 < B_1 < 0$. Since $\gamma(n_0)$ has simple zeroes for $n_0 = B_2$ and $n_0 = B_1$, these points are Hopf bifurcation points. In this section we explore the families of periodic solutions we expect to emerge at the Hopf points B_1 and B_2 and compute the bifurcation curves in the (A, n_0)-plane [2].

Firstly, we study the bifurcation of a branch of periodic solutions and its continuation for varying n_0 for a small fixed value of A. Figure 6^a displays the corresponding bifurcation diagram. It shows that a small amplitude A induce a small region of instability of the on-state where a unique branch of stable SP exists.

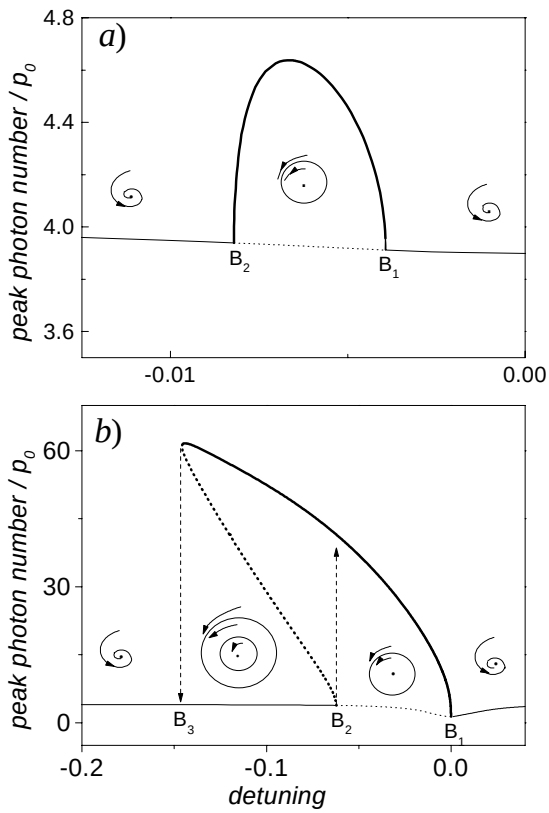

Fig. 6: Bifurcation diagrams of the stable and unstable on-states (thin solid lines and thin doted lines, respectively), and stable (thick solid lines) and unstable (thick doted lines) periodic solutions. The insets show the phase portraits of the two-dimensional system (10)-(11) in the (n, p)-plane. Used parameters: a)$A = 0.015$, b)$A = 1$, and $W = 0.02, \mathcal{J} = 2, \alpha = 5, \Delta = 0.1$.

[2]The bifurcation detection and continuation software package AUTO has been used to perform the numeric computations [16].

(Note the different scaling of the n_0-axis in Fig. 6^a and in Fig. 6^b). Both Hopf points B_1 and B_2 are supercritical.

For larger values of A the bifurcation scenario changes. The corresponding bifurcation diagram is presented in Fig. 6^b. The lower Hopf point B_2 becomes subcritical and a branch of unstable periodic solutions emerges for decreasing n_0. For $n_0 < B_2$ we have the coexistence of a stable steady state, a stable SP and an unstable periodic solution separating the attractors. The branch of the unstable periodic solutions bifurcating from B_2 and the branch of stable SP emanating from B_1 merge in a saddle-node bifurcation at $n_0 = B_3 < B_2$. The subcritical Hopf point B_2 and the saddle-node point B_3 imply a hysteresis phenomenon with jumping behaviour at B_3 and B_2 (depicted by dashed arrows in Fig. 6^b).
Varying both parameters n_0 and A we obtain the Hopf curve P_1-P_2-P_3 in the (A, n_0)-plane where the curve P_1-P_2 is a supercritical Hopf curve and the curve P_2-P_3 is a subcritical Hopf curve (see Fig. 7). At the point P_2 the Hopf bifurcation is degenerated and a branch of saddle-node bifurcations of periodic solutions emerges (the curve P_2-P_4 in Fig. 7). These bifurcation curves divide the parameter plane into three regions. The on-state is the only attractor in region I. In region II the stable on-state and a stable SP coexist and are separated by an unstable periodic solution. The on-state is unstable and the SP is stable in region III. Since point P_3 is near the minimum $A_{\min}$ of the Hopf curve the scenario of Fig. 6^b is predominant for fixed A and varying detuning n_0.
The other RE function parameters influence the bifurcation curves of Figure 7 in the following manner: a decrease of W contracts the regions II and III where P_3 and P_4 are shifted towards P_1. At the same time A_{min} tends to the origin. A change of α or Δ implies only a minor change of the line P_2-P_4.

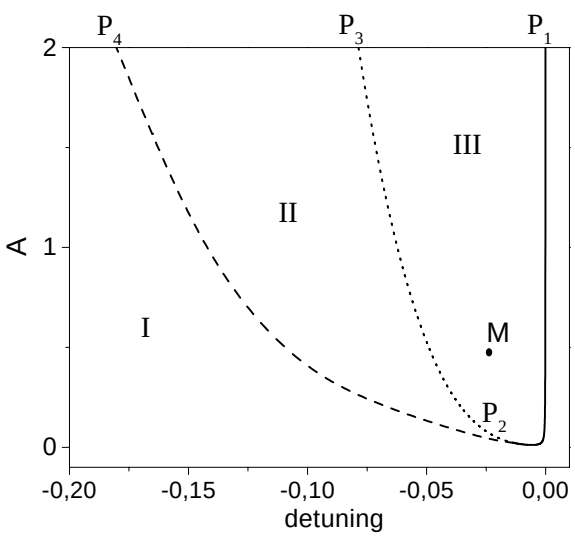

Fig. 7: Decomposition of the (n_0, A)-plane in three regions with different qualitative behaviour, where $W = 0.02, \mathcal{J} = 2$ and $\alpha = 5, \Delta = 0.1$

5 Tuning the SP Frequency and Extinction Ratio

In what follows we are interested in tuning (in the sense of increasing) the frequency of the stable self-pulsations compared with the relaxation frequency $f_0 = \sqrt{T\mathcal{J}}/2\pi$ of the solitary gain section.
Let us first consider the case $\alpha = 0$, $W = 0.05$ and draw the curves of the same frequency and the curves of the same modulation depth in the (A, n_0)-plane.

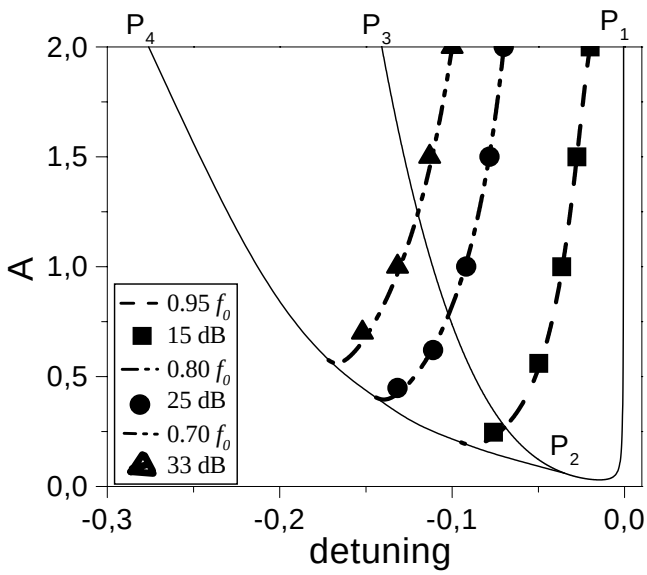

Fig. 8: Isofrequency contours with $\alpha = 0$, $W = 0.05, \mathcal{J} = 2$. The bold contours represent curves with the same frequency of self-pulsations. The big marks indicate the same modulation depth. The modulation depth is measured in terms of dB= $10\log(p_{\max}/p_{\min})$.

Our numerical investigations yield for any W the following results (see Fig. 8):

(i). Each curve of the same frequency is also a curve of the same modulation depth.

(ii). The frequency (modulation depth) monotonically decreases (increases) with increasing distance from the curve of supercritical Hopf bifurcation.

Next we fix a point M in the (A, n_0)-plane (see Fig. 7) and draw the curves of the same frequency and the curves of the same modulation depth in the (α, Δ)-plane (Fig. 9). This picture shows that

(i). frequency and modulation depth increase with increasing α if Δ is sufficiently large, i. e. the interval of gain enhancement covers the variation of n along the orbit of the SP,

(ii). the frequency of the SP is larger than f_0 for $\alpha > 0$.

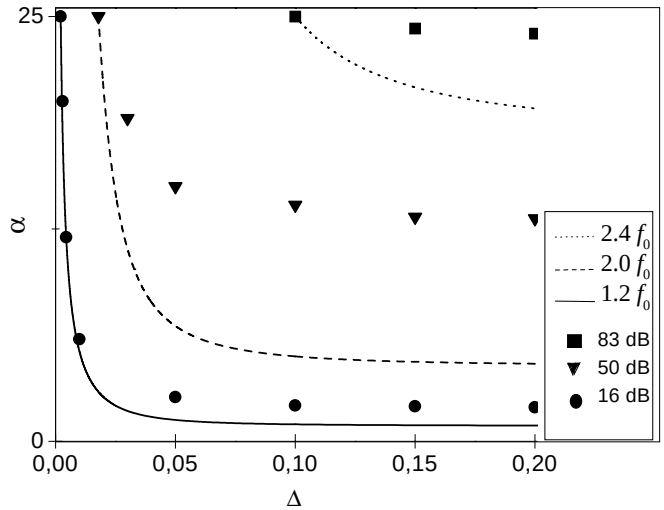

Fig. 9: Contours of constant frequency and modulation depth in the (α, Δ)-plane for parameters $W = 0.02, \mathcal{J} = 2$ and $A = 0.5, n_0 = 0.25$.

6 Summary and Conclusions

In this paper we have investigated numerically a single mode model for PDR lasers. This model represents a two-dimensional system of autonomous ordinary differential equations (rate equations) depending on two crucial functions K and G describing the properties of the PDR. Using a characteristic sample of parameters for a PDR laser we have calculated a typical shape for the functions K and G and have fitted these functions by the expressions (9) and (10). Numerical investigations of the bifurcation scenario and of the phase portrait yield the following results:

The detuning n_0 which determines the position of the resonance of the function K is the essential bifurcation parameter. A typical bifurcation scenario is as follows: For large n_0 the on-state is asymptotically stable. With decreasing n_0 the decay rate enhances for small positive n_0. Near $n_0 = 0$ the decay rate decreases rapidly. The on-state loses its stability by a supercritical Hopf bifurcation and a branch of stable self-pulsations emerges. If n_0 further decreases, the on-state regains its stability by a subcritical Hopf bifurcation and a branch of unstable periodic solutions arises. With decreasing n_0 both branches of periodic solutions merge and disappear in a saddle-node bifurcation.

From the numerical investigations we can derive the following conclusions: A PDR influences the dynamics of a single-mode laser by a narrow resonance-like enhancement of the RE-function K and a local gain enhancement. The amplitude and the position of the resonance of the function K control the existence of self-pulsations and the stability of the on-state. Here, the important question arises how to express n_0 in terms of easily accessible device parameters (see [9] for a first approach). There are parameter constellations where the PDR laser can be used for optical switching. An increase of the frequency of the SP beyond the relaxation frequency of a single

section device can not be obtained by means of the parameters of the function K, however an increasing of the slope of the local gain enhancement allows to reach this goal.

Acknowledgements V. Tronciu acknowledges financial support from Alexander von Humboldt Foundation and Weierstraß Institut Berlin. V.T. expresses his gratitude for the hospitality in the group of Prof. Fritz Henneberger at the Humboldt-Universität zu Berlin, Institut für Physik and in the research group "Dynamical Systems" at the Weierstraß Institut Berlin.

References

[1] M. Möhrle, U. Feiste, J. Hörer, R. Molt, and B. Sartorius, "Gigahertz self-pulsations in 1.5 μm wavelength multisection DFB lasers," *IEEE Photon. Technol. Lett.*, vol. 4, pp. 976-979, 1992.

[2] B. Sartorius, M. Möhrle, and U. Feiste, "12 GHz to 64 GHz continuous frequency tuning in self-pulsating 1.55 μm multi quantum well DFB lasers," IEEE J. of Selected Topics in Quantum Electronics 1, pp. 535-38, 1995.

[3] U. Feiste, D. J. As, and A. Erhardt, "18 GHz all-optical frequency locking and clock recovery using a self-pulsating two-section DFB laser," *IEEE Photon. Technol. Lett.*, vol. 6, pp. 106-108, 1994.

[4] B. Sartorius, M. Möhrle, S. Reichenbacher, and W. Ebert "Controllable self-pulsations in multisection DFB lasers with an integrated phase-tuning section," *IEEE Photon. Technol. Lett.*, vol. 7, no. 11, pp. 1261-1263, 1995.

[5] B. Sartorius, M. Möhrle, and S. Reichenbacher, "Wavelength and polarization independent synchronization of high frequency DFB type self-pulsations", Electron. Lett. 32, pp. 1026-28, 1996.

[6] B. Sartorius, M. Möhrle, and S. Reichenbacher, "Wavelength independent clock recovery at 10 Gb/s using self-pulsating DFB lasers with integrated phase tuning section", Proceedings of ECOC '96.

[7] U. Bandelow, H.-J. Wünsche, and H. Wenzel, "Theory of self-pulsations in two-section DFB lasers," *IEEE Photon. Technol. Lett.*, vol. 5, pp. 1176-1179, 1993.

[8] D. D. Marcenac and J. E. Caroll, "Distinction between multimoded and singlemoded self-pulsations in DFB lasers," *Electron. Lett.*, vol.30, pp. 1137-1138, 1994.

[9] H.-J. Wünsche, U. Bandelow, H. Wenzel, and D.D. Marcenac, "Self pulsations by mode degeneracy in two-section DFB-lasers," *Physics and Simulation of Optoelectronic Devices III*, SPIE vol. 2399, pp. 195-206, 1995.

[10] H. Wenzel, U. Bandelow, H.-J. Wünsche, and J. Rehberg, "Mechanisms of fast self pulsations in two-section DFB lasers," IEEE Journal of Quantum Electronics QE-32, No.1, pp. 69-79, 1996.

[11] B. Sartorius, M. Möhrle, S. Reichenbacher, H. Preier, H.-J. Wünsche, and U. Bandelow "Dispersive self Q-switching in self-pulsating DFB lasers," *IEEE Journ. of Quantum Electronics*, Vol. 33, pp. 211-18, 1997.

[12] U. Bandelow, H.-J. Wünsche, and B. Sartorius, "Dispersive self Q-switching in DFB-lasers: theory versus experiment", IEEE Journal of Selected Topics in Quantum Electronics 3, pp. 270-278, 1997.

[13] U. Bandelow, R. Schatz, and H.-J. Wünsche, "A correct single-mode photon rate equation for multi-section lasers," *IEEE Photon. Technol. Lett.*, vol. 8, pp. 614-617, 1996.

[14] K. Petermann, "Calculated spontaneous emission factor for double-heterostructure injection lasers with gain -induced waveguiding", IEEE J. Quantum Electron., vol. QE-15, pp. 566-70, 1979.

[15] J. Rehberg, H.-J. Wünsche, U. Bandelow, H. Wenzel "Spectral Properties of a System Describing Fast Pulsating DFB Lasers", Z. angew. Math. Mech. 77 1, 75-77, 1997.

[16] E. J. Doedel, A.R. Champneys, T.F. Fairgrieve, Y. A. Kuznetsov, B.Sandstede, X. Wang, "**Auto 97** Continuation and bifurcation software for ordinary differential equations" March 1998.

[17] M. Radziunas, H.-J. Wünsche, B.Sartorius, O. Brox, D. Hoffmann, K.Schneider "Modeling of self-pulsating DFB lasers", Preprint WIAS Berlin, 1999.